Ultrafast Dynamics of Transition Metal Carbonyls. 3. Intracluster Chemistry in $[Cr(CO)_6]_n$

Michael Gutmann,* Markus S. Dickebohm, and Jörg M. Janello

Institut für Physikalische Chemie, Luxemburger Strasse, 116 D-50939 Köln, Germany

Received: October 23, 1998; In Final Form: January 13, 1999

We report on one-color femtosecond−pump/probe experiments applied to homogeneous chromium hexacarbonyl clusters which are prepared in a molecular beam. The pump pulse initiates bimolecular intra-cluster reactions by ultrafast photodissociation of a CO ligand from $Cr(CO)_6$ in a $^1T_{1u}$ metal-to-ligand charge-transfer state. The resulting reaction products are detected mass-selectively after multiphoton ionization by the probe pulse. In contrast to nanosecond multiphoton ionization (Peifer, W. R.; Garvey, J. F. *Int. J. Mass Spectrom. Ion Processes* **1990** *102*, 1), which exclusively leads to appearance of the Cr^+ mass peak, a number of novel species which may serve as interesting model systems for catalysis and surface chemistry are detected. In addition to mononuclear fragments, metal cluster ions, and coordinatively unsaturated polynuclear metal carbonyls, metal oxides and carbides are observed in the femtosecond mass spectra. The appearance of these species can be rationalized by formation of asymmetric π-bridging CO ligands in the neutral manifold. The dynamics extracted from the transients of different reaction products is interpreted using concepts of surface and inorganic cluster chemistry. Ultrafast metal−metal bond formation on a time scale much faster than our laser pulse width (ca. 150 fs) can be observed. Site exchange of CO from terminal to bridging positions on the picosecond time scale is proposed to occur in coordinatively unsaturated polynuclear metal carbonyls. Experiments at different center wavelengths (280 and 262.5 nm) reveal energy-dependent reaction channels which are closed when exciting the clusters at 280 nm. When exciting at 262.5 nm, impulsive formation of the corresponding products and decay on the picosecond time scale is observed.

1. Introduction

The investigation of polynuclear transition metal carbonyls in the gas phase provides an opportunity to study effects ranging from an isolated system of a single metal atom with CO molecules attached to it up to adsorbates on metal surfaces.[1] Of special interest are the binding properties exhibited by those clusters and the dynamics of bond breakage and bond formation. In addition, coordinatively unsaturated transition metal carbonyls and organometallics, for whom transition metal carbonyls serve as model systems, are of great catalytic importance for a number of industrially important processes, e.g. isomerization, oligomerization, and hydration of olefins.[1,2] Metal carbonyls also play an important role in preparing thin metal films via chemical vapor deposition.[3] Thus detailed studies regarding the elementary reaction mechanisms of these cluster systems are of great interest in order to gain insight into their dynamical chemical properties.

Up to now, most investigations on the structure and dynamics of polynuclear transition metal carbonyls have focused on systems which already contain a metal−metal bond. Prototype systems which have been investigated in the gas phase are $Mn_2(CO)_{10}$ and $Re_2(CO)_{10}$ (see, e.g., refs 4−12). These compounds show intense absorption in the region between 330 and 500 nm which is assigned to the $\sigma \rightarrow \sigma^*$ transition of the metal−metal bond.[13] Photoexcitation of this transition leads to homolytic cleavage of the metal−metal bond in competition with ligand dissociation.[9] Leutwyler and Even investigated $Mn_2(CO)_{10}$ and $Fe_3(CO)_{12}$ by nanosecond multiphoton dissociation (MPD)/multiphoton ionization (MPI) using a N_2 -laser pumped dye laser in the region of 380−450 nm.[7] They only observed the bare metal cluster ions Mn^+, Mn_2^+ and Fe^+, Fe_2^+, Fe_3^+, respectively, i.e., 7−10 laser photons had to be absorbed by the parent molecule. Vaida and co-workers observed in their MPI experiments on $M_2(CO)_{10}$ (M = Mn, Re) only M^+ and M_2^+ in the mass spectra.[9,10] Similar to the mononuclear transition metal carbonyls, the polynuclear species exhibit complete ligand stripping in the gas phase under multiphoton conditions when applying nanosecond laser pulses. Real-time studies in solution with femtosecond laser pulses focused on the decarbonylation dynamics and on geminate recombination induced by the solvent cage.[14,15] A landmark study by Zewail and co-workers on $Mn_2(CO)_{10}$ in a molecular beam yielded directly the fragmentation time scales of metal−metal bond cleavage (40 fs) and metal−CO bond breakage (20 fs) when exciting the $\sigma \rightarrow \sigma^*$ transition.[12] Their femtosecond mass spectrum obtained by MPI at 310 nm was strongly dominated by Mn^+ and Mn_2^+ ions. Coordinatively unsaturated binuclear metal carbonyls were of only minor importance.

Formation of coordinatively unsaturated binuclear metal carbonyls in the gas phase has been observed after irradiation of stable mononuclear precursors which after loss of CO ligands undergo bimolecular reactions with additional mononuclear carbonyls.[16−20] A promising source of generating polynuclear coordinatively unsaturated transition metal carbonyls of higher nuclearity may be provided by photoexciting homogeneous mononuclear transition metal carbonyl van der Waals clusters. Smalley, Duncan, and co-workers prepared homogeneous $[Fe(CO)_5]_n$ clusters in a molecular beam which they photoionized at several excimer wavelengths.[21,22] Exciting at 157 nm (one-photon ionization) evidence for cluster formation was given by observation of $[Fe(CO)_5]_n^+$ cluster ions in the mass spectra. At 193 nm, monomer fragments and Fe_n^+ cluster ions up to approximately $n = 30$ were detected. Smaller peaks correspond-

10.1021/jp984206m CCC: $18.00
Published on Web 03/24/1999

ing to multiples of 56 + 28 amu were observed and assigned to coordinatively unsaturated polynuclear iron monocarbonyls. The photofragmentation was shown to take place in the neutral manifold. At 249 nm, the same mass spectra with smaller efficiency were observed. Miller and co-workers built upon this work and performed picosecond-MPI experiments.[23−25] They extended these studies by adding argon or various reactive gases to the $Fe(CO)_5$ clusters and observed a number of different reaction products.

Peifer and Garvey studied homogeneous group VIb transition metal carbonyl clusters, i.e., $[Mo(CO)_6]_n$, $[Cr(CO)_6]_n$, and $[W(CO)_6]_n$, by nanosecond-MPI at 248 nm.[26,27] Due to the quadrupole mass spectrometer employed, they could only detect ions up to 210 amu. Under cluster conditions, Peifer and Garvey observed in addition to the dominating bare metal ions oxidized metal ions in their mass spectra. However, no ions of coordinatively unsaturated transition metal carbonyls were observed. The $[Mo(CO)_6]_n$ clusters yielded MoO^+ and MoO_2^+ and the $[W(CO)_6]_n$ clusters WO^+. For $[Cr(CO)_6]_n$ only Cr^+ was observed, the mass spectrum did not change in going from monomer to cluster conditions. The formation of the oxides was interpreted in terms of a novel bimolecular intracluster reaction occurring within the homogeneous transition metal carbonyl clusters. Structurally, the occurrence of the metal oxides was proposed to result from bridging CO ligands with the O atom attached to one and the C atom attached to another metal atom in the neutral such that these CO ligands formally donate four electrons. The failure to observe any oxidized chromium species in the $[Cr(CO)_6]_n$ experiments was explained by the possibility of forming different structures in these clusters, e.g., a strong tendency to form direct metal−metal bonds. The space available for the valence d-orbitals was cited to explain such a tendency.

From these results it appears to be appropriate to investigate the reaction dynamics of homogeneous $[Cr(CO)_6]_n$ clusters after photoexcitation in more detail. Our ongoing femtosecond real-time experiments are aimed at approaching the following questions: Is it possible to generate unsaturated polynuclear transition metal carbonyl clusters which may serve as model systems for adsorbates on metal surfaces and may lead to novel catalysts? Does there occur novel bimolecular intracluster chemistry? Does reactivity depend on excitation energy? What time scales are involved?

These clusters are ideal precursors for observing bimolecular reactions on the femtosecond time scale as the zero of time which is ill-defined for ordinary full-collision bimolecular reactions can precisely be determined by the photodissociation event initiated by a femtosecond laser pulse. In the pioneering work of Wittig and co-workers and Soep and co-workers, it was realized that van der Waals clusters allow to study full collisions by initiating a unimolecular dissociation reaction producing the reactants within the cluster environment, albeit with restricted impact parameters due to the precursor geometry (for reviews see refs 28−31 and references therein). These experiments naturally paved the way to real-time studies of bimolecular reactions, a field which has been opened up by the famous experiments of Zewail, Wittig, and co-workers on the precursor clusters $HI{\cdot}CO_2$ and $HBr{\cdot}I_2$.[32−37] In the former case photodissociation leads to a hot H atom colliding with CO_2 to yield CO and OH, whereas in the latter case photodissociation leads to a hot Br atom colliding with I_2 to yield IBr and I.

In this contribution we shall present our first attempts toward answering the above questions by applying femtosecond pump/probe spectroscopy to homogeneous $[Cr(CO)_6]_n$ clusters prepared in a molecular beam. We shall show that polynuclear coordinatively unsaturated species of type $Cr_n(CO)_m$ are formed, indeed, under our experimental conditions. In addition, we shall show that novel bimolecular intracluster chemistry can be observed in these clusters leading to detection of oxidic and carbidic metal ions. Time scales of formation and decay of various reaction products will be given from preliminary one-color pump/probe experiments.

The paper is organized as follows: In section 2 we shall briefly describe the experimental setup used for these studies. In section 3 we shall present our results which will be discussed in section 4. The paper will be concluded by section 5.

2. Experimental Section

The experimental setup has been described in detail elsewhere.[38] Briefly, femtosecond pulses of 80−100 fs at center wavelength of 805 nm, ca. 17 mJ pulse energy at a repetition rate of 10 Hz, were derived from a modified commercial femtosecond Ti:Sapphire chirped pulse amplification system (BMI, Alpha 10 series). The amplifier was seeded by an argon ion laser (Coherent, Innova 310) pumped Kerr lens mode-locked Ti:Sapphire oscillator (Coherent, Mira Basic). The amplified pulses were frequency doubled in a 0.5 mm long BBO I crystal yielding pulses of up to 7 mJ pulse energy centered at 402.5 nm. These pulses simultaneously pumped two home-built two-stage white light seeded optical parametric amplifiers (OPAs) whose signal output is tunable in the visible. Typical pulse durations after prism compression were ca. 150 fs ($sech^2$). For the one-color experiments at 280 and 262.5 nm, both OPAs were tuned to center wavelengths of 560 and 525 nm, respectively. Typical crosscorrelation widths routinely measured during the experiments were 250−300 fs ($sech^2$). The output of one OPA was delayed with respect to that of the other one using a Michelson interferometer arrangement via a delay stage (Aerotech, ATS0230 with stepper motor). Both OPA pulses were recombined on a beam splitter and frequency doubled in a 0.2 mm long BBO I crystal. The resulting femtosecond UV pulses were focused into the molecular beam.

For preparation of the homogeneous $[Cr(CO)_6]_n$ clusters we used a molecular beam apparatus consisting of two differentially pumped chambers, a main chamber housing the pulsed solenoid nozzle (General Valve, Series 9 with home-built conical orifice of 200 μm diameter driven by a home-built triggering and driver assembly), which is separated from the buffer chamber by a rhodium plated nickel skimmer (Beam Dynamics) of 1.5 mm diameter. The buffer chamber houses a home-built linear time-of-flight (TOF) mass spectrometer of Wiley−McLaren type[39] with a multichannel plate detector (Hamamatsu, F1552−29S). Neon gas (Linde, 99.995%) at a backing pressure of ca. 4 bar was seeded by $Cr(CO)_6$ (Aldrich, 99%, used as received) heated to approximately 363 K and expanded through the nozzle. The beam ($x/d \sim 100$) entered the second chamber where it was crossed by the laser pulses. Molecular beam, laser pulses, and TOF axis were mutually perpendicular to each other. The pump pulse excited a $^1T_{1u}$ MLCT (metal-to-ligand charge transfer) state of $Cr(CO)_6$ at 262.5 nm (280 nm) which is known to lead to ultrafast dissociation of CO ligands[38,40] and initiated the reaction dynamics. The probe pulse ionized the nascent neutral photofragments by MPI and the resulting ions were detected mass-selectively. Care was taken that the pump beam did not produce any measurable ion signal by itself. After amplification the multichannel plate signal was sent to a digital signal analyzer (Tektronix, DSA 601). At each delay position complete TOF mass spectra were taken which were averaged for typically 100 laser shots. A number of scans (typically about 15) was

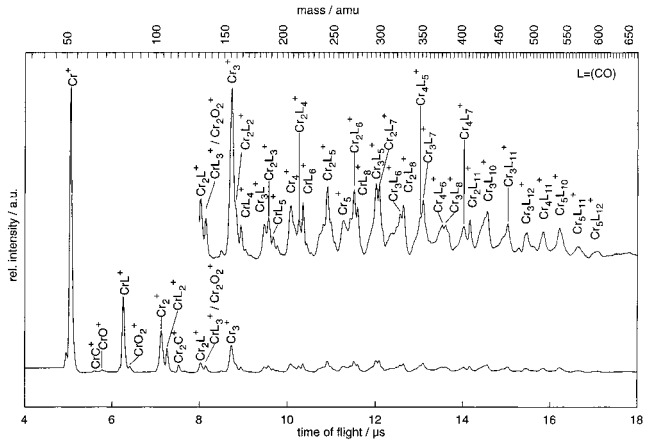

Figure 1. Averaged femtosecond pump/probe mass spectrum of $[Cr(CO)_6]_n$ clusters at center wavelengths of 262.5 nm.

averaged. The average laser intensity was monitored by a photodiode which also served to trigger the DSA in order to check for any irregularities in signal strength. Transients were obtained by integrating each mass peak of interest at each delay position. Data analysis was performed on a DEC Alpha workstation.

3. Results

Mass Spectra. Figure 1 shows a mass spectrum obtained from homogeneous $[Cr(CO)_6]_n$ clusters after pumping a $^1T_{1u}$ MLCT state by femtosecond laser pulses centered at 262.5 nm and probing at the same wavelength. The mass spectrum is averaged over the whole delay range covered (0−130 ps) to show all mass peaks that are observed. The mass spectrum (at each delay time) is clearly dominated by the Cr^+ ion peak but, in sharp contrast to the nanosecond-MPI spectra on $[Cr(CO)_6]_n$ clusters,[27] it is not the only mass peak observed. Instead, the mass spectrum shown in Figure 1 consists of a large number of additional mass peaks which mainly correspond to metal cluster ions Cr_n^+ and polynuclear coordinatively unsaturated metal carbonyl ions $Cr_n(CO)_m^+$ with n going from zero up to at least $n = 5$. The formation of nanoparticles such as the ones we observe in the mass spectrum has been termed "inverse laser ablation" by Miller and co-workers.[24]

In addition, all possible mononuclear metal carbonyl ions $Cr(CO)_m^+$ with $m = 0-6$ are present in the mass spectrum. Similar experiments conducted on $Cr(CO)_6 \cdot (CH_3OH)_k$ heteroclusters[41] only yielded those with $m = 0-3$ and 6; thus, there may exist different cooling efficiencies between these two types of cluster species. Furthermore, some unexpected ions corresponding to metal oxides and metal carbides are observed in the mass spectrum. These ion peaks may hint toward a reactive neutral intermediate that is responsible for a dissociation reaction of CO within the excited cluster environment. Table 1 lists ion peaks from the mass spectrum which can uniquely be assigned.

The polynuclear metal carbonyl cluster ions are coordinatively highly unsaturated (the ion $Cr_5(CO)_{12}^+$ must have lost at least 18 CO ligands in the neutral and ionic manifold together, if we assume the minimum sized precursor cluster $[Cr(CO)_6]_5$; the presence of the Cr_5^+ metal cluster indicates that in order to form this ion the parent cluster must even have lost 30 CO ligands). The neutral reaction products after excitation of the homogeneous clusters by the pump pulse are most likely less unsaturated polynuclear metal carbonyl clusters which upon ionization by the probe pulse lose further CO ligands and van der Waals bound $Cr(CO)_6$ units. The fact that the mass spectrum is

TABLE 1: Mass Peaks Identified in the Mass Spectrum Shown in Figure 1

ion	*m*/*z* (amu)	ion	*m*/*z* (amu)
Cr^+	52	Cr_5^+	260
CrC^+	64	$Cr_2(CO)_6^+$	272
CrO^+	68	$Cr(CO)_8^+$	276
$Cr(CO)^+$	80	$Cr_3(CO)_5^+$	296
CrO_2^+	84	$Cr_2(CO)_7^+$	300
Cr_2^+	104	$Cr_3(CO)_6^+$	324
$Cr(CO)_2^+$	108	$Cr_2(CO)_8^+$	328
Cr_2C^+	116	$Cr_4(CO)_5^+$	348
$Cr_2(CO)^+$	132	$Cr_3(CO)_7^+$	352
$Cr(CO)_3^+$	136	$Cr_4(CO)_6^+$	376
$Cr_2O_2^+$ [a]	136	$Cr_3(CO)_8^+$	380
Cr_3^+	156	$Cr_4(CO)_7^+$	404
$Cr_2(CO)_2^+$	160	$Cr_2(CO)_{11}^+$	412
$Cr(CO)_4^+$	164	$Cr_3(CO)_{10}^+$	436
$Cr_3(CO)^+$	184	$Cr_3(CO)_{11}^+$	464
$Cr_2(CO)_3^+$	188	$Cr_3(CO)_{12}^+$	492
$Cr(CO)_5^+$	192	$Cr_4(CO)_{11}^+$	516
Cr_4^+	208	$Cr_5(CO)_{10}^+$	540
$Cr_2(CO)_4^+$	216	$Cr_5(CO)_{11}^+$	568
$Cr(CO)_6^+$	220	$Cr_5(CO)_{12}^+$	596
$Cr_2(CO)_5^+$	244		

[a] Isobaric with $Cr(CO)_3^+$.

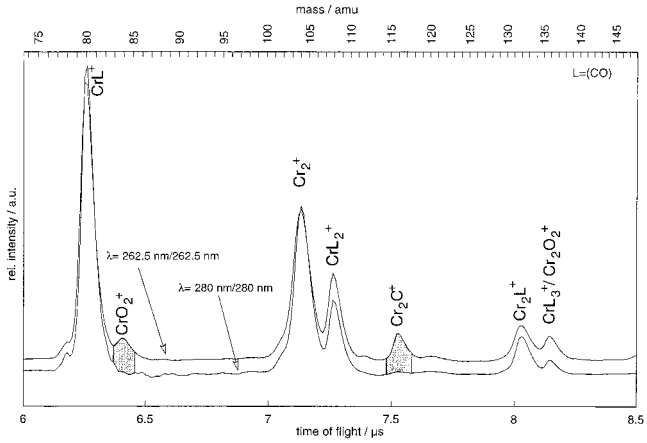

Figure 2. Comparison of averaged $[Cr(CO)_6]_n$ femtosecond pump/probe mass spectra taken at different center wavelengths.

dominated by bare metal cluster ions Cr_n^+ may already point to the possibility that metal−metal bond formation is a driving force in the intracluster reactions taking place in the neutral manifold. It is interesting to note that with increasing nuclearity the relative number of CO ligands per Cr atom appears to decrease when looking at the least unsaturated cluster ions.

Mass spectra obtained at 280 nm pump/probe center wavelengths are very similar to the one shown in Figure 1. However, some important differences are present. In Figure 2 a comparison between portions of mass spectra recorded at 262.5 nm pump/probe center wavelengths and 280 nm pump/probe center wavelengths is shown. When comparing the mass peaks corresponding to CrO_2^+ and Cr_2C^+ it is readily observed that these ions appear only in the mass spectrum obtained at higher pump/probe photon energies. From these findings it can be deduced that formation of the neutral reaction products leading to these ions upon probing appears to be dependent on the excess energy deposited initially. The corresponding reaction channels are obviously closed at 280 nm.

Transients. Figure 3 gives an overview of the time-dependent measurements by pseudo-three-dimensional plots of several transients obtained with femtosecond pulses at 262.5 nm pump/probe center wavelengths up to 65 ps. Mass peaks corresponding to different ion flight times are indicated in the figure. On the

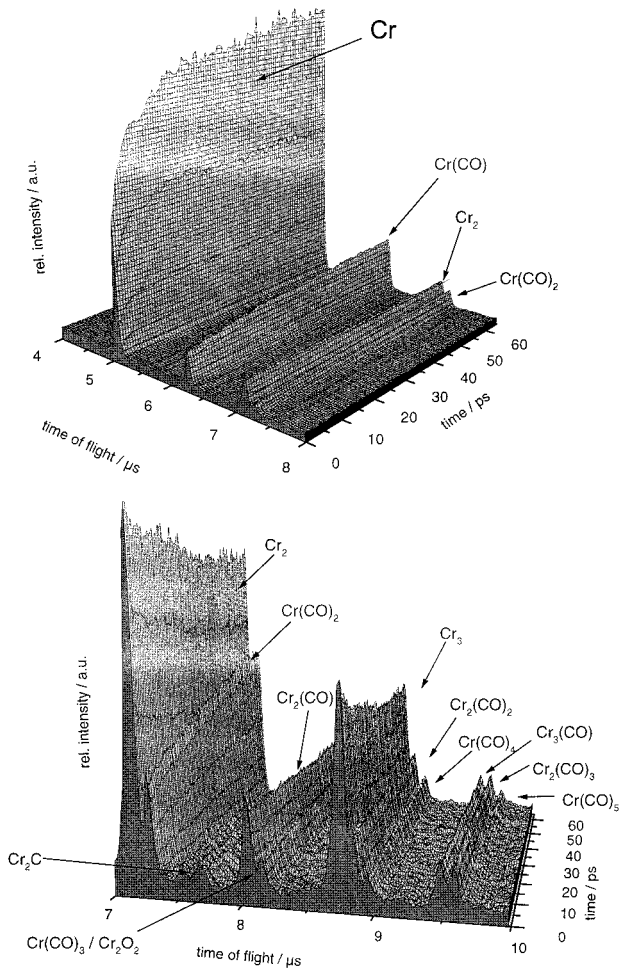

Figure 3. Pseudo-three-dimensional plots of experimental transients obtained at pump/probe center wavelengths of 262.5 nm.

left-hand side of Figure 3 transients measured at the most intense ion signals (Cr^+, $Cr(CO)^+$, $Cr(CO)_2^+$, Cr_2^+) are shown, the right-hand side of Figure 3 contains transients obtained at less intense ion signals. From the figure qualitative conclusions can be drawn: All transients corresponding to mononuclear ion peaks show monotonically rising behavior on the picosecond time scale whereas those corresponding to metal cluster and polynuclear coordinatively unsaturated cluster ions decrease toward a constant asymptotic level on the picosecond time scale after fast initial rises. It should be noted that $Cr(CO)_3$ is isobaric with Cr_2O_2, so interferences of transients leading to both of these ions are possible (vide infra).

To obtain a more detailed view of the dynamics going on in the clusters, in what follows some cuts through the hypersurfaces shown in Figure 3 will be presented. The experimental transients were measured up to a delay time of 130 ps; the step width chosen during the first 6 ps was 66 fs, and for the remainder of the transients it was 1.33 ps. In Figure 4 a transient obtained at the Cr^+ ion signal is shown together with fits to a single exponential rise (left) and to a triple exponential rise (right) and the corresponding residuals. The fits were obtained by convoluting the model function (here: single exponential rise and triple exponential rise, respectively) with a Gaussian of experimental crosscorrelation width. From the figure it can clearly be deduced that a single-exponential rise does not fit the experimental transient well. The residuals show systematic deviations from zero and the short time part of the transient cannot be represented by the fit at all. The triple exponential rise shows much better agreement with the experimental transient even though the first rise time of 180 fs appears to be too long due to the transient peak at about 250 fs which cannot be fit properly. It seems obvious that several time scales are involved in the dynamics of the neutral reaction product corresponding to the chromium ion signal. Figure 5 shows the $CrCO^+$ transient together with a fit to a triple exponential rise. It should be noted that the first rise time (T1 = 63 fs) can only be taken as a rough estimate due to our time resolution and the step width chosen. In addition to a very fast initial rise this transient exhibits a peak after about 250 fs which is probably due to the initial fast dissociation dynamics of $Cr(CO)_6$ within the clusters. Similar transient peaks have been observed for the decarbonylation dynamics of $Cr(CO)_6$ in the gas phase[38,40] and in $Cr(CO)_6 \cdot (CH_3OH)_k$ heteroclusters.[41] In Table 2 the rise times T3 describing the long time part of the transients of the coordinatively most unsaturated mononuclear chromium carbonyl ions are listed for both experiments conducted at pump/probe center wavelengths of 262.5 nm and 280 nm. A rise time for the $Cr(CO)_3^+$ transient is only given for the experiments conducted at 280 nm since these do not exhibit interferences with an isobaric species as will be explained below.

Figure 6 shows Cr_n^+ transients on both a short time scale and a longer time scale. The rise and decay times obtained from fits to a triple exponential rise (Cr^+), a biexponential rise and single-exponential decay (Cr_2^+), and a single-exponential rise and single-exponential decay (Cr_3^+, Cr_4^+) are given in Table 3. The fits included convolution with a Gaussian of experimental crosscorrelation width as described above. Rise times T1 which are shorter than 150 fs have to be taken only as estimates due to our time resolution and the experimental step size. After fast initial rise the transients exhibit peaks after ca. 250 fs indicating fast passage through a very short-lived state induced by the primary photodissociation event. The Cr_2^+ transient exhibits a late maximum after about 20 ps followed by a picosecond decay toward an asymptotic minimum. In contrast, the Cr_3^+ and Cr_4^+ transients after a fast initial rise decay monotonically on a picosecond time scale. Higher chromium cluster transients are similar to the latter two transients. Only the Cr_2^+ transient exhibits the peak after 20 ps. From the figure it is apparent that the neutral reaction products giving rise to the metal cluster ions upon interaction with the probe pulse are formed extremely fast (pulse width limited rise times are observed in our experiments) and decay on a picosecond time scale. Results from the experiments conducted at 280 nm pump/probe center wavelengths are also given in Table 3. These latter experiments yielded essentially pulse width limited rise times followed by a decay indicated by times T3 in the table. The Cr_2^+ and Cr_3^+ transients decay on the same time scale for both wavelength pairs, the Cr_4^+ transient decays much faster for pump/probe center wavelengths of 280 nm.

The signal intensities obtained at the mass peaks of the coordinatively unsaturated carbonyl ions $Cr_n(CO)_m^+$ were quite low, so the transients measured did not allow for a detailed quantitative analysis. However, the main features could easily be deduced and the transients are presented in order to provide a more complete picture of the dynamics going on in the $[Cr(CO)_6]_n$ clusters after photoexcitation by the pump pulse. Additional experiments aimed at quantifying the characteristic rise and decay times require a considerably better signal-to-noise ratio which can only be obtained by improving the experimental setup. These experiments will be performed in our laboratory soon. In Figure 7 as an example a transient measured at the Cr_2CO^+ mass peak (pump/probe center wavelengths: 262.5 nm) is shown together with a fit to a single-exponential

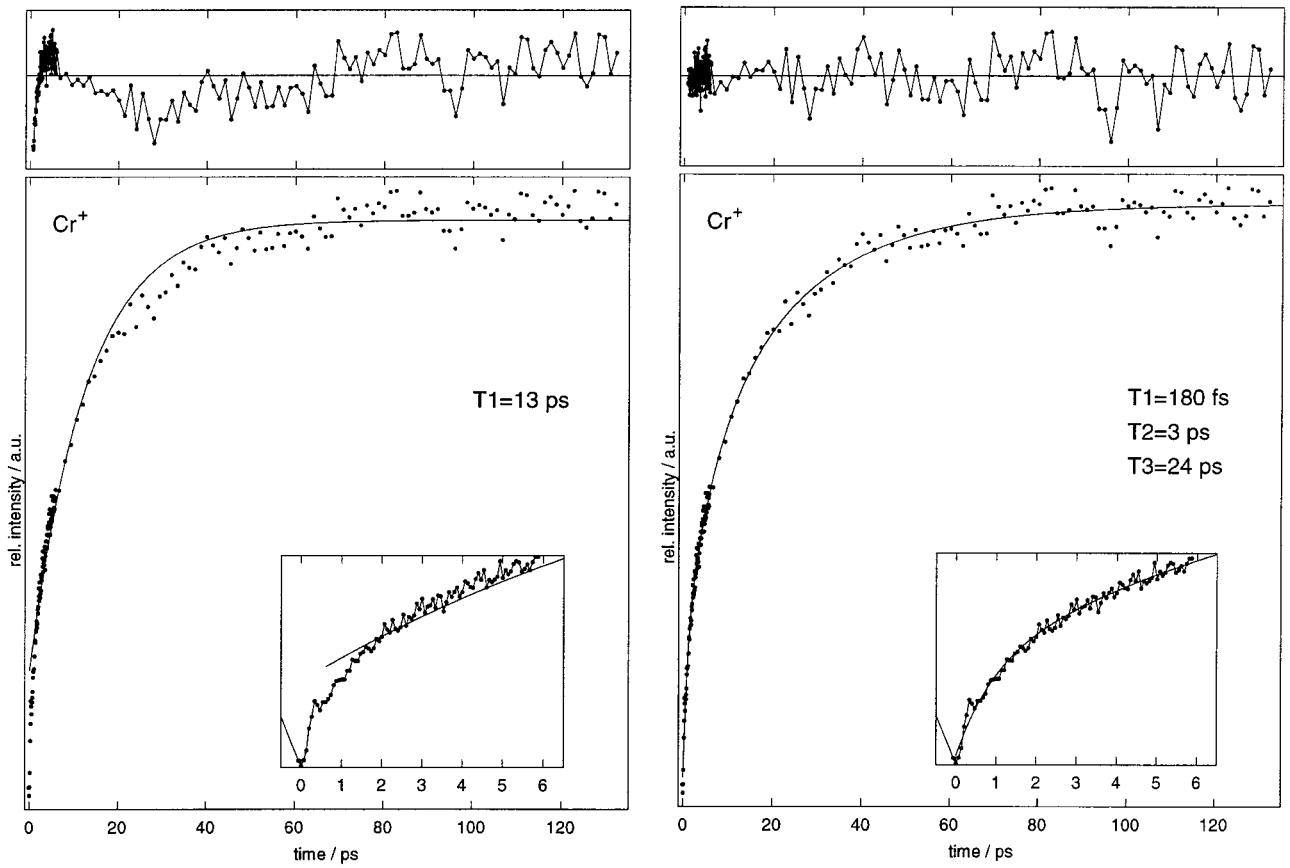

Figure 4. Cr^+ transient obtained at pump/probe center wavelengths of 262.5 nm together with fits to exponential rise functions after convolution with a Gaussian of experimental crosscorrelation width. Residuals are shown in the upper frames. The inserts correspond to a shorter time scale up to 6 ps. Rise times are indicated in the figure. Left: fit to a single-exponential rise (rise time T1). Right: fit to a triple exponential rise (rise times T1, T2, T3).

rise and a single-exponential decay. The transient exhibits a pronounced peak after ca. 250 fs similar to the peaks observed in the transients presented above. Like the Cr_2^+ transient a peak after ca. 20 ps is reached which is followed by a decay on the picosecond time scale. However, the rise time of 20 ps is different from that observed in the Cr_2^+ transient. To obtain a better view at the structure of the $Cr_2(CO)_m^+$ transients we removed high-frequency noise by applying a low pass filter to the transients after Fourier transfom. The window function chosen was a Gaussian. The results after back transforming the filtered transients measured at pump/probe center wavelengths of 262.5 nm and those obtained at pump/probe center wavelengths of 280 nm are shown in Figure 8. Gray bars denote the approximate positions of the maxima. Fits to single exponential rises and single exponential decays are also shown for guiding purposes. Comparison of the maxima in Figure 8 shows an essentially constant shift of about 4 ps toward longer delay times for the $Cr_2(CO)_m^+$ ($m = 0-4$) transients in going from m to $m + 1$ (262.5 nm). The exact position of the maxima is rather difficult to determine since the peaks are quite flat. The maximum of the $Cr_2(CO)_5^+$ transient is slightly shifted back toward shorter delay times and those of the $Cr_2(CO)_{6,7}^+$ transients are again shifted toward longer delay times in going from m to $m + 1$ by about 1 ps. A similar behavior is exhibited by the transients measured at 280 nm; however, the maxima appear much earlier, those of the $Cr_2(CO)_m^+$ ($m = 0-3$) transients nearly instantaneously. The shifts of the maxima indicate that the dynamics detected at the mass positions of different polynuclear carbonyl ions mainly derive from different neutral precursors which result from the intramolecular reactions induced by the pump pulse. It is unlikely that these precursors are formed by simple CO ligand dissociation since in that case one would expect the maxima to shift to later delay times in going from m to $m - 1$ instead of going from m to $m + 1$ as is clearly observed here. Transients measured at metal carbonyl ion peaks of higher nuclearity show the same general appearance as those presented in Figure 8, they are, however, contaminated by more noise, so we decided not to show them here.

Figure 9 shows transients obtained at mass peaks of CrO^+ and CrC^+ for both pump/probe center wavelengths. Rise times obtained from fits to a single-exponential rise are indicated in the figure and are all on in the picosecond range. These transients do not show any specific structure on the femtosecond time scale. Thus, formation of the corresponding neutral products does not appear to be directly coupled to the initial fast reaction. The transients reach asymptotic maxima and must correspond to a neutral reaction product which is at least stable for the time covered by our experiments (130 ps). The only possible source of oxygen and carbon within the homogeneous clusters are CO ligands which must be dissociated either in the neutral or ionic manifold. Peifer and Garvey observed metal oxides in their ns-MPI studies on homogeneous transition metal carbonyl clusters only for the tungsten and molybdenum species but not for the chromium ones.[27] In Figure 10 corresponding transients obtained at the CrO_2^+ and Cr_2C^+ mass peaks (pump/probe center wavelengths: 262.5 nm) are shown. Both of these transients decay on the picosecond time scale after fast initial rise which is in contrast to the transients shown in Figure 9. The CrO_2^+ transient exhibits a (convoluted) rise time of 90 fs (single exponential) and a single-exponential decay time of 36 ps. Due to the pronounced peak after 250 fs, a rise time for the Cr_2C^+ transient could not be determined, the decay fits well to

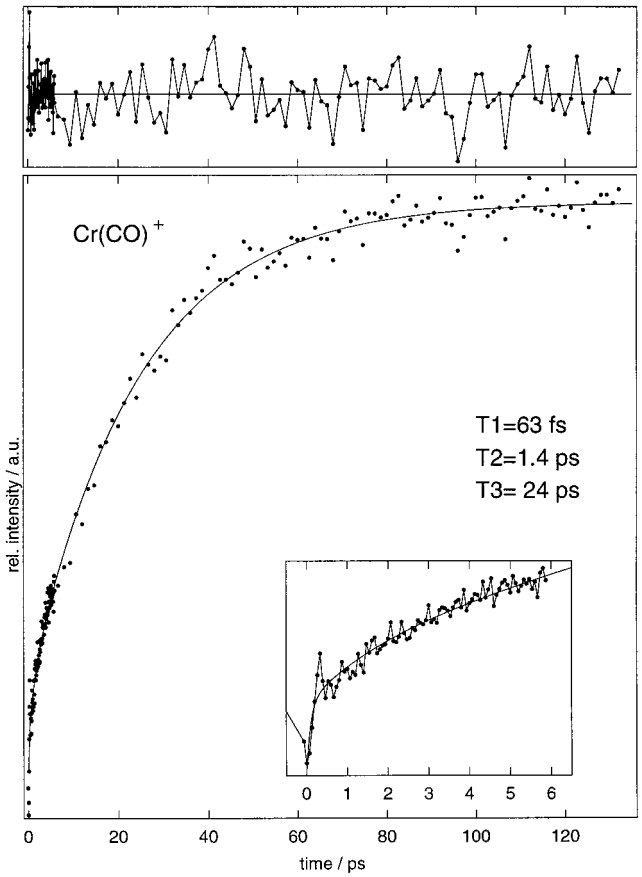

Figure 5. $CrCO^+$ transient obtained at pump/probe center wavelengths of 262.5 nm together with a fit to a triple exponential rise after convolution with a Gaussian of experimental crosscorrelation width and corresponding residuals. Rise times (T1, T2, T3) are indicated in the figure. The insert corresponds to a shorter time scale up to 6 ps.

TABLE 2: Comparison of the Long-Time Rise Times of the Transients Obtained for Some Mononuclear Chromium Carbonyl Ions at Different Center Wavelengths

fragment	262.5 nm rise time T3 (ps)	280 nm rise time T3 (ps)
Cr^+	24 ± 3	20 ± 1
$Cr(CO)^+$	24 ± 1	26 ± 1
$Cr(CO)_2^+$	50 ± 3	43 ± 2
$Cr(CO)_3^+$		19 ± 2

a biexponential with characteristic decay times of 5 and 74 ps, respectively.

At mass 136 amu we may identify two isobaric species, $Cr(CO)_3$ and Cr_2O_2. Figure 11 shows the transients measured at the 136 amu mass signals for both center wavelengths. If the signal at 136 amu was entirely due to $Cr(CO)_3^+$, a transient exhibiting a monotonic rise on the picosecond time scale would be expected by comparing it with those obtained from the remaining mononuclear chromium carbonyl ions. However, the transient measured at pump/probe center wavelengths of 262.5 nm shows a single exponential rise followed by a single exponential decay which is not the expected behavior. It thus appears quite likely that an isobaric species ($Cr_2O_2^+$) deriving from a different neutral reaction product leads to interference with the $Cr(CO)_3^+$ transient. This is confirmed when comparing the corresponding transient measured at pump/probe center wavelengths of 280 nm. This transient exhibits the expected monotonic rise. It may thus be concluded that the reaction leading to the neutral precursor of the $Cr_2O_2^+$ ion does not take place at 280 nm, similar to what was observed for CrO_2^+ (vide supra).

4. Discussion

To gain a better understanding of the possible processes going on in the homogeneous clusters after photoexcitation by the pump pulse, a short discussion of the relevant energetic data of the $Cr(CO)_6$ monomer may be in order. In Figure 12 excitation energies, ionization energies, and bond dissociation energies (BDE's) obtained from literature data are given. The ionization energy of $Cr(CO)_6$ and its ionic BDE's are taken from ref 42, the ionization energy of Cr is taken from ref 43. First and second neutral BDE's of $Cr(CO)_6$ are taken from ref 44, the third BDE from ref 45, and the other neutral BDE's are obtained by dividing the remaining dissociation energy of the process $Cr(CO)_6 \rightarrow Cr + 6CO$ by three, similar to an estimate proposed in ref 46. Solid arrows in the figure denote the photon energies corresponding to the center wavelength of 262.5 nm. Energy uncertainties as quoted in the cited references are denoted by the shaded areas.

As can be seen from the figure, a single pump photon is sufficient to excite a $^1T_{1u}$ MLCT state[47] of $Cr(CO)_6$ which is followed by ultrafast ligand dissociation to form electronically excited $Cr(CO)_5$ in the ^1E state.[38,40] Electronically excited $Cr(CO)_5$ is proposed to rapidly undergo internal conversion to the vibrationally hot electronic ground state within less than 100 fs, followed by further dissociation of a CO ligand.[38,40] These observations were in line with a sequential decarbonylation model of $Cr(CO)_6$ in the gas phase.[45] The energetic position of the $Cr(CO)_5$ ^1E state as obtained from condensed phase experiments[48] is also indicated in Figure 12. Two-photon absorption by the parent $Cr(CO)_6$ leads into the ionic manifold. Thus, the dynamics we shall discuss below cannot arise from two-photon absorption by a parent $Cr(CO)_6$ unit within the homogeneous cluster since the pump pulse was not able to produce any significant ion signal as discussed in section 2. It must either be induced by a single pump photon leading into the $^1T_{1u}$ state of $Cr(CO)_6$ or by absorption of an additional photon from the pump pulse by a photofragment formed within the pulse width.

Before discussing the dynamical processes which may occur in the homogeneous clusters after photoexcitation some remarks on possible neutral reaction products leading to the ions observed in our experiments (see Figure 1) will be made. Since the species we observe are novel compounds whose structures are not known experimentally and have not yet been calculated theoretically, we have to rely on what is known about stable polynuclear transition metal carbonyl compounds and relevant surface chemistry in the literature. As the mass spectra are dominated by metal cluster ions and coordinatively unsaturated polynuclear metal carbonyl cluster ions, it can be assumed that formation of metal−metal bonds appears to be favored in the intracluster reactions. Bridging CO ligands may assist in further strengthening the metal−metal bonds. The bond formation then yields excess energy which can be disposed of by dissociation of additional CO ligands.

The presence of chromium oxide and carbide ions in the mass spectra points to the existence of asymmetrically bridging CO ligands where the carbon atom is bound to one chromium atom and the oxygen atom to a neighboring one. Peifer and Garvey discussed π-bonding (d−π^* back-bonding) CO molecules to explain the appearance of tungsten oxide and molybdenum oxide ions in their nanosecond-MPI mass spectra.[26,27] They based their arguments on experiments by Shinn and Madey who observed

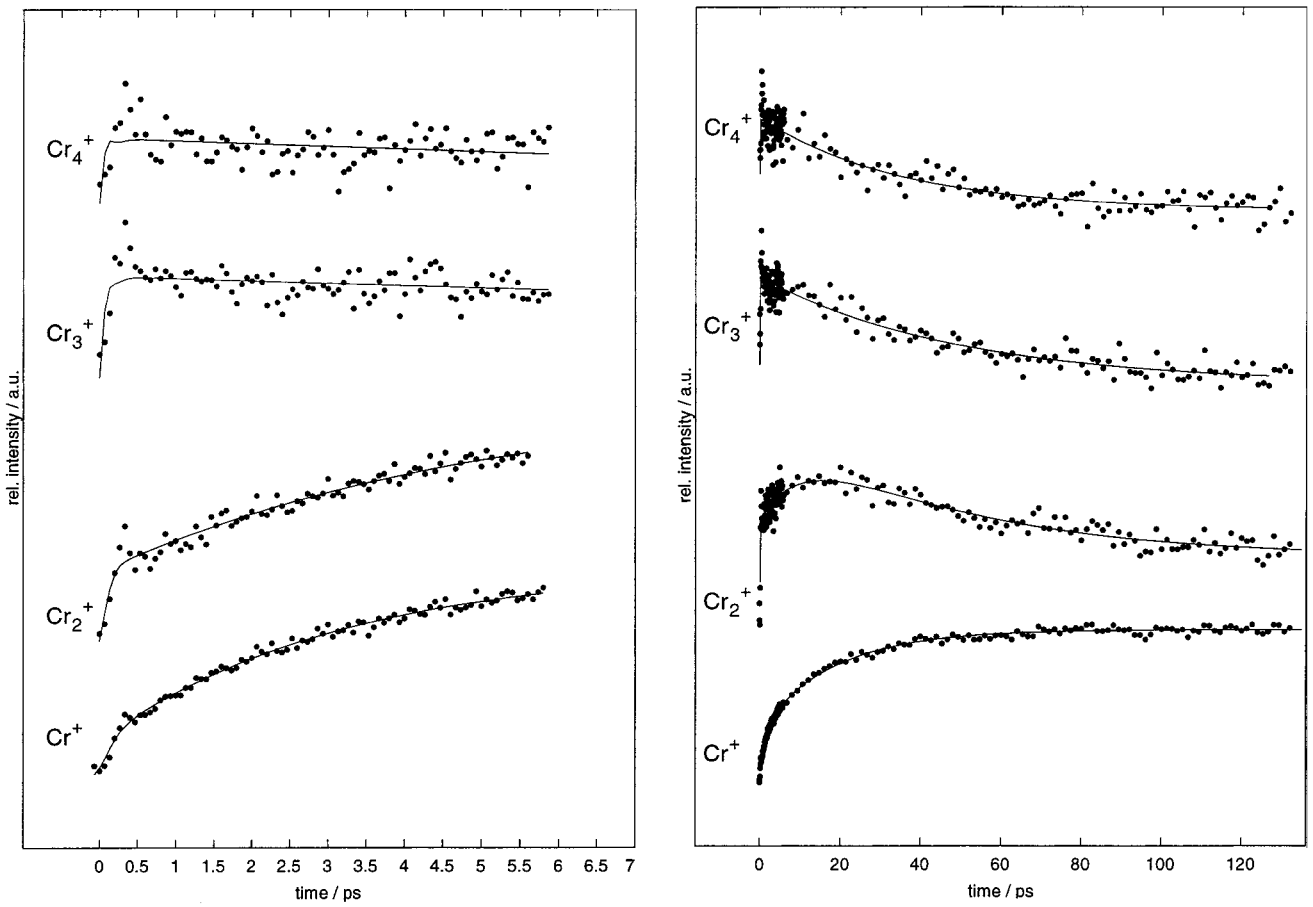

Figure 6. Comparison of Cr_n^+ ($n = 1-4$) transients obtained at pump/probe center wavelengths of 262.5 nm. Left: Transients on a short time scale up to 6 ps. Right: Transients on a longer time scale up to 130 ps.

TABLE 3: Rise Times and Decay Times (underlined) of the Cr_n^+ ($n = 0-4$) Transients Obtained from Fits (for Details, See Text)[a]

fragment	time constant T1 (fs)	time constant T2 (ps)	time constant T3 (ps)
Cr^+	180 ± 10	3 ± 0.5	24 ± 3
Cr_2^+	130 ± 14	5 ± 0.5	$\underline{45 \pm 14}$
Cr_3^+	50 ± 8		$\underline{51 \pm 3}$
Cr_4^+	50 ± 40		$\underline{35 \pm 8}$

[a] Errors given are uncertainties due to the fits and do not correspond to the actual time resolution of our experiments.

two types of CO molecules adsorbed on a Cr[110] surface.[49] In these surface experiments an α_1-CO species at low coverage could be detected which was explained to be π-bound with the intramolecular axis oriented parallel to the surface. The authors showed that α_1-CO is a precursor to CO dissociation on the surface. From these results it appears reasonable to assume that the oxidic and carbidic chromium ions observed in our mass spectra derive from a similar neutral precursor which must have formed after absorption of the pump pulse by the homogeneous $[Cr(CO)_6]_n$ clusters. Further support comes from the literature on stable polynuclear transition metal carbonyls where the existence of asymmetrically bridging CO ligands was shown.[50-52] An example is the compound $[(\eta^5\text{-}C_5H_5)Mo(CO)_2]_2$. The bonding mechanism has been explained by charge donation from a metal d-orbital to the CO π*-orbital similar to what has been proposed for α_1-CO.[49]

The appearance of highly unsaturated polynuclear metal carbonyl ions and metal cluster ions indicates that a considerable amount of energy must be available in the clusters in the ionic and/or neutral manifold. Assuming for an order of magnitude estimate an average BDE of 9000 cm^{-1}, formation of Cr_5^+ involves a total of 270,000 cm^{-1} of energy corresponding to more than seven photons at 262.5 nm if starting with the smallest cluster possible, i.e., $[Cr(CO)_6]_5$. As discussed above, $Cr(CO)_6$ within a neutral cluster absorbs one photon from the pump pulse which means that not more than 3 (in case of absorption of an additional pump photon by a primary photofragment which in principle is possible as most of the transients measured show pulse width limited rise times: 6−7) CO ligands will be dissociated if intracluster processes leading to additional excess energy do not occur. If this is assumed then up to 27 (20−21) ligands must be lost in the ionic manifold after absorption of the (strong) probe pulse which needs more than six probe photons. This number may become slightly smaller due to the fact that the ionization energies of the cluster species will be lower than that of the unclustered photofragments. Unfortunately, those data are at present unavailable. However, since we observe a large number of metal carbonyl ions of different degree of coordinative saturation in our pump/probe mass spectra which are of comparable signal intensity, it seems unlikely that all of these ions arise from (statistical) fragmentation in the ionic channel. In addition, if that was the case and the ions observed derived mainly from dissociation after absorption of the probe pulse, most of the transients obtained at different ionic peak positions should show the same dynamic behavior. This is not the case as can be seen from the transients shown in section 3 which clearly differ from each other. It appears thus most likely that different reaction products are formed in the neutral after the pump event which leads to additional excess energy available for CO dissociation. From

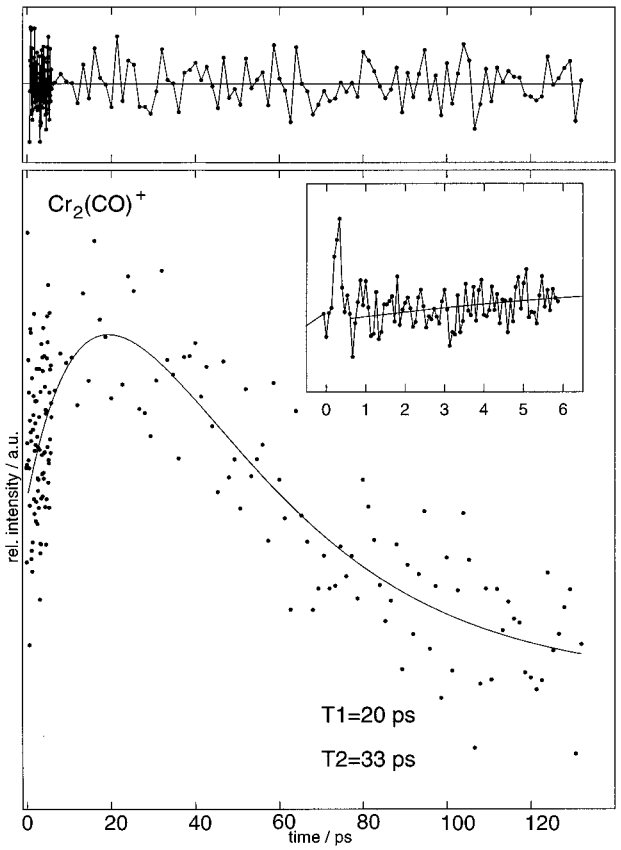

Figure 7. Cr_2CO^+ transient obtained at pump/probe center wavelengths of 262.5 nm together with a fit to a single-exponential rise and single-exponential decay and corresponding residuals. Rise (T1) and decay (T2) times are indicated in the figure. The insert corresponds to a shorter time scale up to 6 ps.

the dominance of the metal cluster ions in the mass spectra, metal−metal bond formation to form a metal framework at which CO molecules are adsorbed seems to be an important process in this respect. Formation of a metal framework will lead to some energy release (the Cr−Cr binding energy in the Cr_2 dimer amounts to 12400 ± 500 cm^{-1} (D_0))[53] possibly leading to CO dissociation and evaporation of van der Waals bound $Cr(CO)_6$ units. The nearly instantaneous rise observed in most of the transients measured in our experiments implies an ultrafast bond forming mechanism which is only possible if the carbonyl cluster units are arranged such that they are close in proximity to the metal−metal bonding distance. This ultrafast bond formation can then be considered as the reverse of ultrafast metal−metal bond fission observed by Zewail and co-workers in $Mn_2(CO)_{10}$.[12] Formation of metal−metal multiple bonds is also well-known in polynuclear cluster compounds.[54] Furthermore, formation of bridging ligands from the terminally bound CO molecules in the octahedral complexes $Cr(CO)_6$ can also lead to additional excess energy as they may be bound more strongly than terminal ligands. In surface chemistry it is known that CO adsorbates are able to occupy edge bridging or face bridging sites on metal surfaces in addition to on top positions.[55] Thus, isomerization processes may be involved in the reaction dynamics. Evidence for bridging ligands is provided by appearance of oxidic and carbidic chromium species in our mass spectra (vide supra). This kind of site exchange isomerization dynamics will involve a high degree of mobility of the CO ligands within the polynuclear clusters. That this assumption is not unreasonable, especially when considering the availability of a considerable amount of excess energy after the pump event and possible metal−metal bond formation, can be seen from the literature: Site exchange has been observed, for example, in $[(\eta^5\text{-}C_5H_5)Fe_2(CO)_4]$.[56] High mobility of CO ligands in polynuclear clusters has also been associated with so-called fluxional clusters where it has been shown that only ligands such as CO which are capable of bridging show fluxional behavior involving rapid exchange of positions.[57] The appearance of different isomers at different times will lead to time-dependent ionization probabilities upon absorption of the time-delayed probe pulse which will be reflected in the transients observed. Thus, the different transients of polynuclear species shown in section 3 may indeed result from this kind of dynamics (vide infra).

Since the results we present in this contribution are the first of an intracluster reaction occurring in $[Cr(CO)_6]_n$ clusters, there is as yet no additional information on possible reactions available, neither from experiment nor from theory. At present, backed by surface experiments and polynuclear cluster chemistry from the literature cited above, we can thus only speculate on the intracluster chemistry going on in our van der Waals clusters. If the primary reaction after absorption of the pump pulse is essentially unaffected by the cluster environment (for $Cr(CO)_6 \cdot (CH_3OH)_k$ this is most likely the case)[41] the photodissociation product $Cr(CO)_5$ which is formed within the pump pulse width could readily react with a neighboring $Cr(CO)_6$ molecule to form solvated $Cr_2(CO)_{11}$, an 18-electron system.[50] This kind of bimolecular reaction has also been proposed to take place in the gas phase.[17,18] It is interesting to note that the highest coordinated binuclear chromium carbonyl ion we can clearly identify in our mass spectrum is $Cr_2(CO)_{11}^+$. This kind of reaction may be the initial process responsible for the intracluster chemistry observed. However, as the transients obtained from metal clusters (see Figure 6) of higher nuclearity rise on a femtosecond time scale, formation of the whole metal framework must occur extremely fast. The figure also indicates that clusters of higher nuclearity are less stable than those of lower nuclearity. This can be seen from the asymptotic value of the transients after 130 ps and from the second rise time of the Cr_2^+ transient as compared to the very fast rising $Cr_{3,4}^+$ ones. This can be explained by the additional excess energy available in the neutral precursors of higher nuclearity since formation of the metal framework will undoubtedly yield a considerable amount of energy becoming available for dissociation. In addition, the bound ion states of the polynuclear compounds will decrease in energy with increasing nuclearity which means that upon probe ionization more excess energy is available for dissociation of the cluster.

Figure 8 shows that the picosecond dynamics of the corresponding neutral polynuclear carbonyls cannot be explained by simple consecutive CO ligand dissociation. If this was the case, it would be expected that transients corresponding to higher coordinated species show maxima at earlier times than those corresponding to coordinatively more unsaturated species. This is clearly not the case when inspecting the transients shown for both center wavelengths. In addition we observe the surprising fact that the dynamics measured at 280 nm center wavelengths appears to occur faster than at 262.5 nm center wavelengths. This is again unexpected for a simple Cr−CO bond fission which should occur faster with increasing available energy. A possible explanation for the latter behavior may be that an endothermic reaction occurs at 262.5 nm which due to the necessary activation energy is not possible at 280 nm. Such a reaction could be formation of the neutral precursors of the CrO_2^+, Cr_2C^+ (and $Cr_2O_2^+$) ions observed in our mass spectra

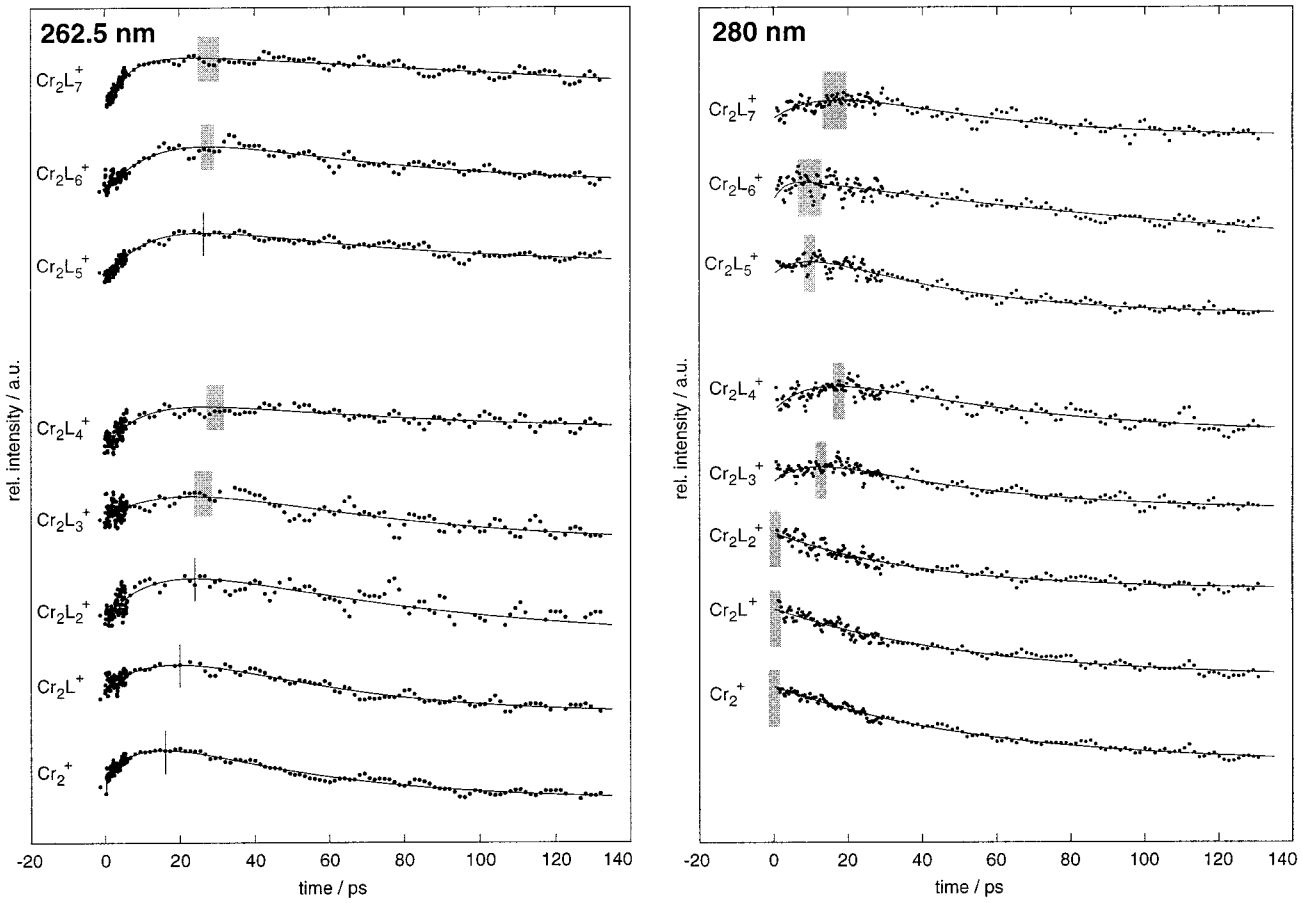

Figure 8. $Cr_2(CO)_m^+$ ($m = 0-7$) transients obtained at pump/probe center wavelengths of 262.5 nm (left) and 280 nm (right). Gray bars denote approximate peak positions on the picosecond time scale.

upon 262.5 nm probe ionization. These ions were not observed at 280 nm. As the transients measured at these mass peaks (Figure 10) show a femtosecond rise and a picosecond decay, the reactions leading to the corresponding neutral species is over when the picosecond dynamics leading to the shifted maxima shown in Figure 8 sets in. The transients exhibit a peak at early times similar to all other transients showing fast femtosecond rises. As similar peaks have been attributed to the initial photodissociation process leading to hot ground-state $Cr(CO)_5$,[38,40,41] we may conclude that the neutral reaction products whose transients show such a peak are connected to these fast photodissociation products, i.e., they are formed in a more or less impulsive way.

The scenario just described does, however, not explain why the less coordinated species show earlier maxima on the picosecond time scale than higher coordinated ones and why the maximum of the $Cr_2(CO)_5^+$ transient shifts back to earlier times. An explanation for this behavior may be formation of bridged ligands by terminally bound ligands moving to different coordination sites. Available energy must be used to break the terminal Cr−CO bond and deliver kinetic energy for mobility which may readily lead to ligand dissociation. If this happens, at early times upon probe ionization less coordinated ionic fragments will be observed. At later times formation of the new bonds occurs. The mobility of ligands can be connected to the fluxionality of polynuclear clusters containing CO ligands.[57] Additional evidence is provided by formation of neutral precursors leading to CrO^+ and CrC^+ ions upon probe ionization. The transients corresponding to these mass peaks (Figure 9) at both center wavelengths exhibit a rise on the picosecond time scale. These transients do not show a transient peak at early times which points to the fact that they are not directly connected to the initial ligand dissociation event. It may thus be possible that these products are formed after movement of a CO ligand to a π-bridging site. It should be noted that molecular rearrangement to form bridged CO ligands can be very fast, indeed, as has been observed in the work of Zewail and coworkers.[12] These authors found that when photolyzing $Mn_2(CO)_{10}$ with femtosecond laser pulses the nascent $Mn_2(CO)_9$ photofragment bridges within 160 fs.

At present we have no explanation for the observation that the maxima of the $Cr_2(CO)_5^+$ transients shift to earlier times with respect to those of the $Cr_2(CO)_4^+$ transients. It may be that those ions arise due to fragmentation from higher neutral cluster species which differ from those corresponding to $Cr_2(CO)_m^+$ ($m \leq 4$).

The rise times of the mononuclear $Cr(CO)_m^+$ ($m = 0-3$) transients given in Table 2 derive from different sources. Part of the rise on the femtosecond time scale may be due to the decarbonylation dynamics of the monomeric $Cr(CO)_6$ as discussed in refs 38 and 40. However, since the Cr_n^+ transients (see Figure 6) with higher n already decay on the femtosecond time scale, their neutral precursors also contribute. The rise of the mononuclear $Cr(CO)_m^+$ ($m = 0-3$) transients on the picosecond time scale may then derive from evaporation of $Cr(CO)_6$ clusters of solvated mononuclear photofragments similar to what has been observed for the $Cr(CO)_6 \cdot (CH_3OH)_k$ heteroclusters in ref 41. However, additional contributions from the picosecond decay of the neutral photoproducts corresponding to the Cr_n^+ and the $Cr_n(CO)_m^+$ ions will be present. It is interesting to note that the rise times T3 of the $Cr(CO)_n^+$ ($n = 0-3$) transients do not differ much when comparing for both

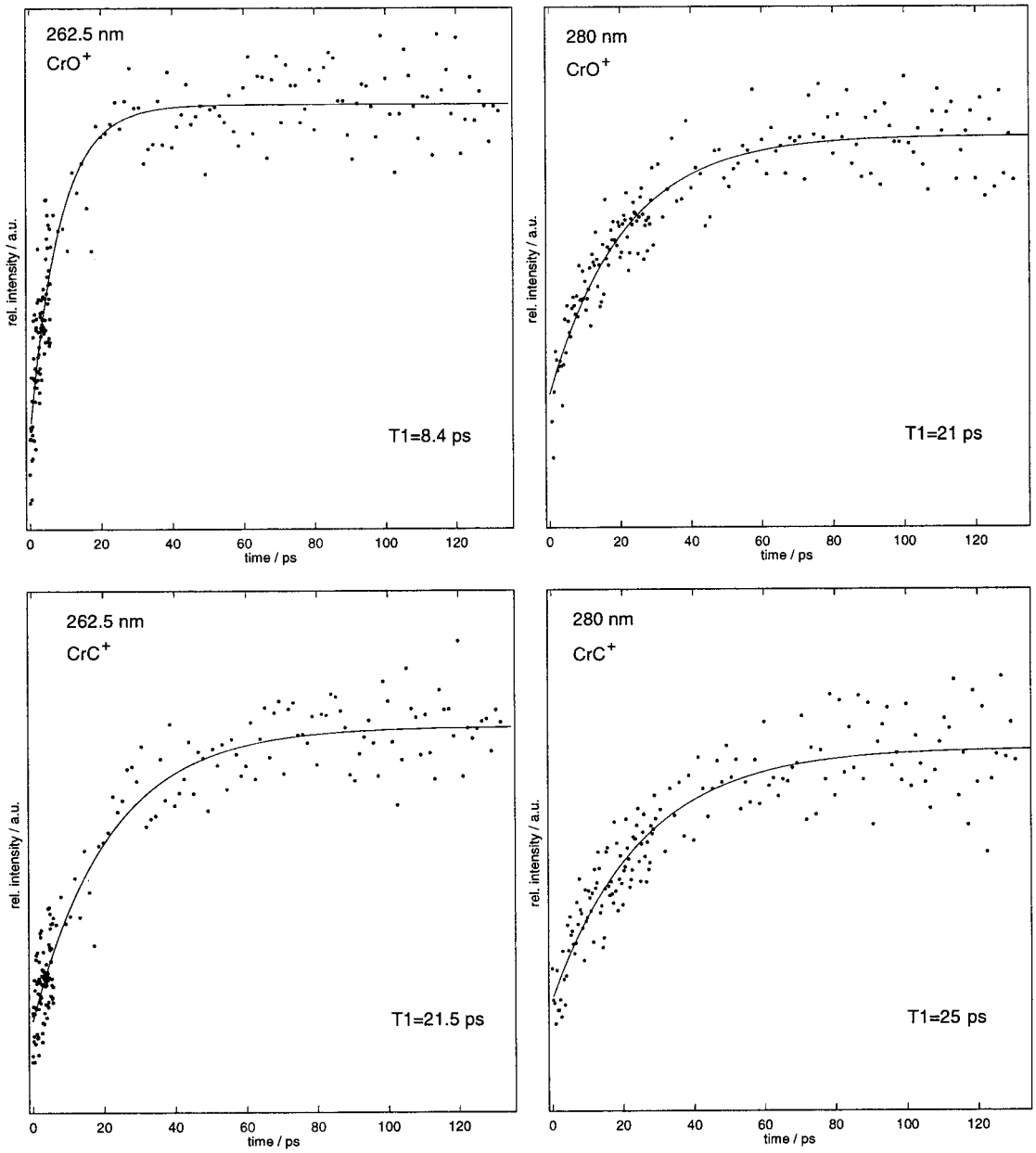

Figure 9. CrO^+ and CrC^+ transients obtained at pump/probe center wavelengths of 262.5 nm (left) and 280 nm (right) together with fits to a single-exponential rise. Rise times (T1) extracted from the fits are indicated.

center wavelengths. This is totally different from our observations for the $Cr(CO)_6 \cdot (CH_3OH)_n$ heteroclusters where the picosecond rise times had been attributed to solvent evaporation. The corresponding rise times at 280 nm were about 90 ps[41] and at 262.5 nm they were between 33 ps and 50 ps.[58] This may again be a hint toward a higher amount of excess energy being available for evaporation of $Cr(CO)_6$ units from the clusters after bond formation, here.

It is still surprising that in the nanosecond-MPI mass spectra of $[Cr(CO)_6]_n$ no ions indicative of cluster formation could be found.[27] Since several species which give rise to the ions observed in the mass spectra obtained in this work live for at least 130 ps, it seems unlikely that short lifetimes are sufficient to explain their absence from the nanosecond-MPI mass spectra. However, since all photoproducts observed in this work are formed on the femtosecond and picosecond time scale, it is quite likely that they readily absorb further photons from an exciting nanosecond-laser pulse which leads to further fragmentation until only the bare chromium atom remains. Thus, in the nanosecond-MPI mass spectrum of $[Cr(CO)_6]_n$, Cr^+ is the only observable ion. However, it is still puzzling that in the nanosecond-MPI mass spectra of other homogeneous group VIb clusters ($[Mo(CO)_6]_n$, $[W(CO)_6]_n$) metal oxide ions indicative of bimolecular intracluster reactions have been observed.[26,27] It appears that $[Cr(CO)_6]_n$ plays a special role among the group VIb clusters. Further femtosecond experiments on the intracluster dynamics of $[Mo(CO)_6]_n$ and $[W(CO)_6]_n$ are planned in our laboratory in order to answer that question.

5. Conclusions

In this contribution we presented our first results on ultrafast intracluster bimolecular chemistry occurring in homogeneous transition metal carbonyl clusters. With femtosecond pulses we obtained a number of novel polynuclear reaction products which upon probe pulse ionization manifest themselves as metal cluster ions Cr_n^+, coordinatively unsaturated polynuclear metal ions $Cr_n(CO)_m^+$, and metal oxides and carbides. These compounds may serve as model systems for polynuclear coordinatively

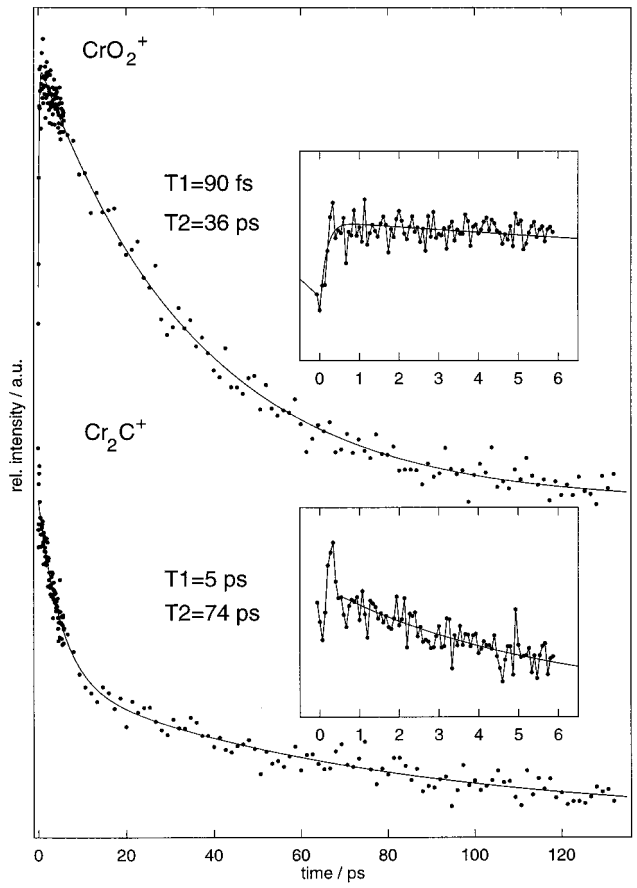

Figure 10. CrO_2^+ and Cr_2C^+ transients obtained at pump/probe center wavelengths of 262.5 nm. Fits to a single-exponential rise (rise time T1) and a single-exponential decay (decay time T2) after convolution with a Gaussian of experimental crosscorrelation width (CrO_2^+) and to a biexponential decay (Cr_2C^+) starting at the maximum (decay times T1, T2) are shown. Inserts correspond to a shorter time scale up to 6 ps.

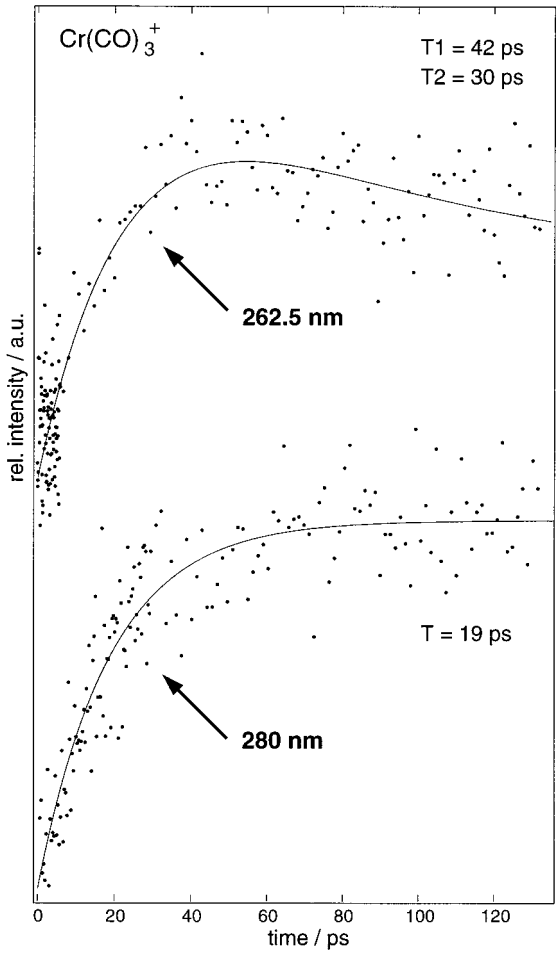

Figure 11. Transients obtained at mass 136 amu with pump/probe center wavelengths of 262.5 nm and 280 nm. Fits to a single-exponential rise and a single-exponential decay (262.5 nm; rise time T1, decay time T2) and to a single-exponential rise (280 nm; rise time T) are shown.

unsaturated transition metal catalysts and surfaces containing adsorbed CO molecules. In contrast to our femtosecond experiments, nanosecond-MPI studies on $[Cr(CO)_6]_n$ clusters exclusively yielded Cr^+ ions. The fact that we observe chromium oxides and carbides in the mass spectra could be explained by formation of a π-bound asymmetrically bridging CO molecule, a species which has also been observed on Cr[110] surfaces and in inorganic polynuclear transition metal cluster compounds.

By following the dynamics of various reaction products on the femtosecond and picosecond time scale, we obtained hints toward possible reaction paths. Pulse-width limited formation of several polynuclear species led us to propose metal−metal bond formation as a major driving force taking place immediately after CO dissociation from a van der Waals-bound $Cr(CO)_6$ unit. Bond formation provides additional excess energy which can be disposed of by CO ligand loss and $Cr(CO)_6$ evaporation. On the picosecond time scale shifted maxima of the transients measured at the coordinatively unsaturated polynuclear chromium carbonyl masses were observed. We could interpret these shifts in terms of isomerization processes such as site exchange of terminally bound CO ligands to form bridging species. The fact that the CrO^+ and CrC^+ transients exhibit similar picosecond rise times could be explained by movement of a CO ligand to a π-bound asymmetric bridging site. This kind of site exchange could be connected to the so-called fluxional clusters known from the literature. It would be highly desirable to calculate possible structures of these coordinatively unsaturated polynuclear transition metal carbonyls and their isomers in order to test our ideas on ultrafast site exchange.

Surprisingly it was found that most transients measured at lower photon energy (pump/probe center wavelengths: 280 nm) exhibited faster dynamics than those measured at higher photon energy (pump/probe center wavelengths: 262.5 nm) even though the excited electronic state was still the same $^1T_{1u}$ state. These findings could be explained by the fact that at higher photon energy additional reaction products could be observed which upon probe ionization showed up as different oxides and carbides, e.g., CrO_2^+, Cr_2C^+. These additional products are formed within our experimental pulse width which means that less energy is left for other competing reactions as compared to the reactions at lower excitation energy where this channel of reaction is closed.

Additional experiments are planned to be performed in our laboratory very soon to elucidate the rich and fascinating intracluster chemistry of transition metal compounds in more detail. Especially, experiments similar to those presented here on $[Mo(CO)_6]_n$ and $[W(CO)_6]_n$ are necessary to explain why $[Cr(CO)_6]_n$ does not show any evidence for intracluster reaction products on the ns time scale whereas the molybdenum and tungsten species do. Experiments employing much shorter pulse widths than the ones presently available to us will be important to elucidate the mechanism of the extremely fast product formation observed in detail. In addition, carefully varying the

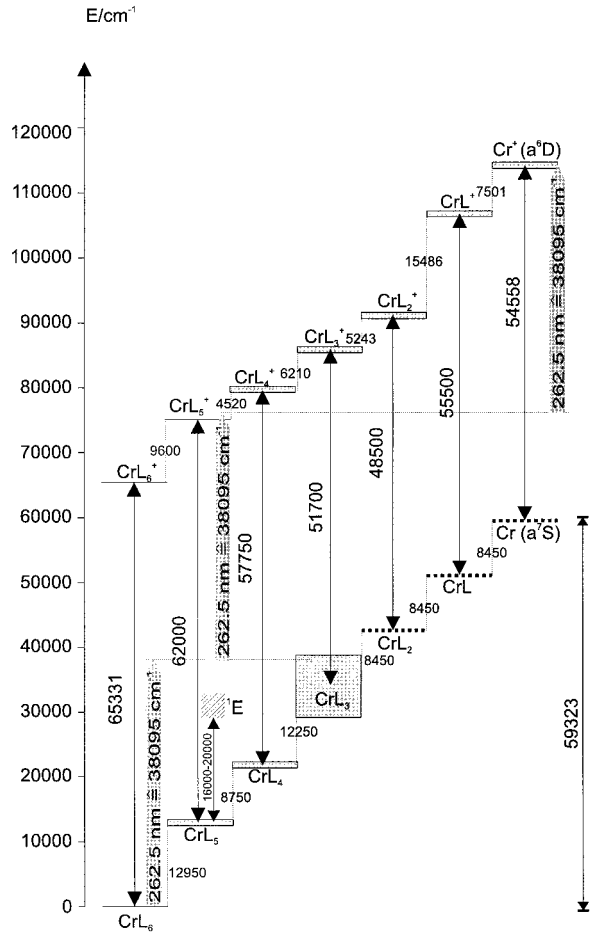

Figure 12. Energetics of $Cr(CO)_6$ dissociation in the neutral and ionic manifold as obtained from literature data (see text for details). Solid arrows indicate photon energies corresponding to 262.5 nm.

expansion conditions of the molecular beam in a reproducible manner may help to clarify the dependence of the time scales of the dynamics involved on cluster size. Finally, two-color experiments with various pump and probe wavelengths will provide more information on the fragmentation pathways in both the neutral and ionic manifold and tell us more about energy-dependent reactions in those complex and fascinating systems.

Acknowledgment. Financial support by the Deutsche Forschungsgemeinschaft (Grants Gu 280/3 and Gu 280/4) via the Schwerpunktprogramme "Molekulare Cluster" and "Femtosekundenspektroskopie elementarer Anregungen in Atomen, Molekülen und Clustern" is gratefully acknowledged. One of us (M.S.D.) wishes to thank the Fonds der Chemischen Industrie for a graduate fellowship. We also thank Prof. G. Hohlneicher for continuous support.

References and Notes

(1) Thimmappa, B. H. S. *Coord. Chem. Rev.* **1995**, *143*, 1.
(2) Yamamoto, A. *Organotransition Metal Chemistry. Fundamental Concepts and Applications*; Wiley: New York, 1986.
(3) Jackson, R. L. In *Laser Microfabrication*; Ehrlich, D. J., Tsao, J. Y., Eds.; Academic Press: New York, 1989.
(4) Hennig, H.; Thomas, P.; Wagener, R.; Rehorek, D.; Jurdeczka, K. *Z. Chem.* 1977 *17*, 241.
(5) Wrighton, M. S.; Ginley, D. S. *J. Am. Chem. Soc.* **1975**, *97*, 2065.
(6) Freedman, A.; Bersohn, R. *J. Am. Chem. Soc.* **1978**, *100*, 4116.
(7) Leutwyler, S.; Even, U. *Chem. Phys. Lett.* **1981**, *84*, 188.
(8) Meyer, T. J.; Caspar, J. V. *Chem. Rev.* **1985**, *85*, 187.
(9) Leopold, D. G.; Vaida, V. *J. Am. Chem. Soc.* **1984**, *106*, 3720.
(10) Hollingsworth, W. E.; Vaida, V. *J. Phys. Chem.* **1986**, *90*, 1235.
(11) Rothberg, L. J.; Cooper, N. J.; Peters, K. S.; Vaida, V. *J. Am. Chem. Soc.* **1982**, *104*, 3546.
(12) Kim, S. K.; Pederson, S.; Zewail, A. H. *Chem. Phys. Lett.* **1995**, *233*, 500.
(13) Levenson, R. A.; Gray, H. B. *J. Am. Chem. Soc.* **1975**, *97*, 6042.
(14) Waldman, A.; Ruhman, S.; Shaik, S.; Sastry, G. N. *Chem. Phys. Lett.* **1994**, *230*, 110.
(15) Schwartz, B. J.; King, J. C.; Zhang, J. Z.; Harris, C. B. *Chem. Phys. Lett.* **1993**, *203*, 503.
(16) Fletcher, T. R.; Rosenfeld, R. N. *J. Am. Chem. Soc.* **1985**, *107*, 2203.
(17) Breckenridge, W. H.; Stewart, G. M. *J. Am. Chem. Soc.* **1986**, *108*, 364.
(18) Seder, T. A.; Church, S. P.; Weitz, E. *J. Am. Chem. Soc.* **1986**, *108*, 4721.
(19) Weitz, E. *J. Phys. Chem.* **1987**, *91*, 3945.
(20) Ganske, J. A.; Rosenfeld, R. N. *J. Phys. Chem.* **1989**, *93*, 1959.
(21) Duncan, M. A.; Dietz, T. G.; Smalley, R. E. *J. Am. Chem. Soc.* **1981**, *103*, 5245.
(22) Wheeler, R. G.; Duncan, M. A. *J. Phys. Chem.* **1986**, *90*, 3876.
(23) Bililign, S.; Feigerle, C. S.; Miller, J. C. *J. Phys. Chem. A* **1997**, *101*, 4569.
(24) Bililign, S.; Feigerle, C. S.; Miller, J. C. *Appl. Surf. Sci.* **1998**, *127*−*129*, 344.
(25) Bililign, S.; Feigerle, C. S.; Miller, J. C.; Velegrakis, M. *J. Chem. Phys.* **1998**, *108*, 6312.
(26) Peifer, W. R.; Garvey, J. F. *J. Phys. Chem.* **1989**, *93*, 5906.
(27) Peifer, W. R.; Garvey, J. F. *Int. J. Mass Spectrom. Ion Processes* **1990**, *102*, 1.
(28) Wittig, C.; Zewail, A. H. In *Chemical Reactions in Clusters*; Bernstein, E. R., Ed.; Oxford University Press: New York; 1996; p 64.
(29) Jouvet, C.; Solgadi, D. In *Chemical Reactions in Clusters*; Bernstein, E. R., Ed.; Oxford University Press: New York; 1996; p 100.
(30) Buelow, S.; Noble, M.; Radhakrishan, G.; Reisler, H.; Wittig, C.; Hancock, G. *J. Phys. Chem.* **1986**, *90*, 1015.
(31) Breckenridge, W. H.; Jouvet, C.; Soep, B. *J. Chem. Phys.* **1986**, *84*, 1443.
(32) Scherer, N. F.; Khundkar, L. R.; Bernstein, R. B.; Zewail, A. H. *J. Chem. Phys.* **1987**, *87*, 1451.
(33) Scherer, N. F.; Sipes, C.; Bernstein, R. B.; Zewail, A. H. *J. Chem. Phys.* **1990**, *92*, 5239.
(34) Gruebele, M.; Sims, I. R.; Potter, E. D.; Zewail, A. H. *J. Chem. Phys.* **1991**, *95*, 7763.
(35) Sims, I. R.; Gruebele, M.; Potter, E. D.; Zewail, A. H. *J. Chem. Phys.* **1992**, *97*, 4127.
(36) Ionov, S. I.; Brucker, G. A.; Jaques, C.; Valachovic, L.; Wittig, C. *J. Chem. Phys.* **1992**, *97*, 9486.
(37) Ionov, S. I.; Brucker, G. A.; Jaques, C.; Valachovic, L.; Wittig, C. *J. Chem. Phys.* **1993**, *99*, 6553.
(38) Gutmann, M.; Janello, J. M.; Dickebohm, M. S.; Grossekathöfer, M.; Lindener-Roenneke, J. *J. Phys. Chem. A* **1998**, *102*, 4138.
(39) Wiley, W. C.; McLaren, I. H. *Rev. Sci. Instrum.* **1955**, *26*, 1150.
(40) Trushin, S. A.; Fuss, W.; Schmid, W. E.; Kompa, K. L. *J. Phys. Chem. A* **1998**, *102*, 4129.
(41) Gutmann, M.; Janello, J. M.; Dickebohm, M. S. *Chem. Phys.* **1998**, *239*, 317.
(42) Qi, F.; Yang, X.; Yang, S.; Gao, H.; Sheng, L.; Zhang, Y.; Yu, S. *J. Chem. Phys.* **1997**, *107*, 4911.
(43) Lide, D. R., Ed.; *Chemical Rubber Company Handbook of Chemistry and Physics*, 75th ed.; CRC Press: Boca Raton, FL, 1994.
(44) Fletcher, T. R.; Rosenfeld, R. N. *J. Am. Chem. Soc.* **1988**, *110*, 2097.
(45) Venkataraman, B.; Hou, H.; Zhang, Z.; Chen, S.; Bandukwalla, G.; Vernon, M. *J. Chem. Phys.* **1990**, *92*, 5338.
(46) Peifer, W. R.; Garvey, J. F. *J. Chem. Phys.* **1991**, *94*, 4821.
(47) Beach, N. A.; Gray, H. B. *J. Am. Chem. Soc.* **1968**, *90*, 5713.
(48) Perutz, R. N.; Turner, J. J. *J. Am. Chem. Soc.* **1975**, *97*, 4791.
(49) Shinn, N. D.; Madey, T. E. *J. Chem. Phys.* **1985**, *83*, 5928.
(50) Spessard, G. O.; Miessler, G. L. *Organometallic Chemistry*; Prentice-Hall: Upper Saddle River, NJ, 1997.
(51) Ginley, D. S.; Wrighton, M. S. *J. Am. Chem. Soc.* **1975**, *97*, 3533.
(52) Klingler, R. J.; Butler, W.; Curtis, M. D. *J. Am. Chem. Soc.* **1975**, *97*, 3535.
(53) Simard, B.; LebeaultDorget, M. A.; Marijnissen, A.; terMeulen, J. J. *J. Chem. Phys.* **1998**, *108*, 9668.
(54) Crabtree, R. H. *The Organometallic Chemistry of the Transition Metals*; Wiley: New York, 1994.
(55) Bradshaw, A. M. *Surf. Sci.* **1982**, *11/12*, 712.
(56) Evans, J.; Johnson, B. F. G.; Lewis, J.; Matheson, T. W. *J. Chem. Soc. Chem. Commun.* **1975**, 576.
(57) Johnson, B. F. G.; Benfield, R. E. *J. Chem. Soc., Dalton Trans.* **1978**, 1554.
(58) Gutmann, M.; Janello, J. M.; Dickebohm, M. S., unpublished results.